REGULAR ARTICLE

Tatjana Haenggi · Marcus C. Schaub ·
Jean-Marc Fritschy

Molecular heterogeneity of the dystrophin-associated protein complex in the mouse kidney nephron: differential alterations in the absence of utrophin and dystrophin

Abstract The dystrophin-associated protein complex (DPC) consisting of syntrophin, dystrobrevin, and dystroglycan isoforms is associated either with dystrophin or its homolog utrophin. It is present not only in muscle cells, but also in numerous tissues, including kidney, liver, and brain. Using high-resolution immunofluorescence imaging and Western blotting, we have investigated the effects of utrophin and dystrophin gene deletion on the formation and membrane anchoring of the DPC in kidney epithelial cells, which co-express utrophin and low levels of the C-terminal dystrophin isoform Dp71. We show that multiple, molecularly distinct DPCs co-exist in the nephron; these DPCs have a segment-specific distribution and are only partially associated with utrophin in the basal membrane of tubular epithelial cells. In utrophin-deficient mice, a selective reduction of β2-syntrophin has been observed in medullary tubular segments, whereas α1-syntrophin and β1-syntrophin are retained, concomitant with an upregulation of β-dystroglycan, β-dystrobrevin, and Dp71. These findings suggest that β2-syntrophin is dependent on utrophin for association with the DPC, and that loss of utrophin is partially compensated by Dp71, allowing the preservation of the DPC in kidney epithelial cells. This hypothesis is confirmed by the almost complete loss of all DPC proteins examined in mice lacking full-length utrophin and all C-terminal dystrophin isoforms (utrophin$^{0/0}$/mdx^{3Cv}). The DPC thus critically depends on these proteins for assembly and/or membrane localization in kidney epithelial cells.

T. Haenggi · M. C. Schaub (✉) · J.-M. Fritschy
Institute of Pharmacology and Toxicology, University of Zurich,
Winterthurerstrasse 190,
8057 Zurich, Switzerland
e-mail: schaub@pharma.unizh.ch
Tel.: +41-1-6355919
Fax: +41-1-6356874

Introduction

The dystrophin-associated protein complex (DPC) is a multimeric membrane-spanning complex linked either to dystrophin, a large X-linked cytoskeletal protein, or to its autosomal homolog utrophin (Matsumura et al. 1992). In skeletal muscle cells, the DPC is composed of α-dystroglycan (an extracellular protein bound to laminin), β-dystroglycan and sarcoglycans (spanning the membrane), and dystrobrevins and syntrophins (located intracellularly). Utrophin and dystrophin anchor this complex to the cytoskeleton by binding to the intracellular tail of β-dystroglycan and to actin filaments (Way et al. 1992; Winder et al. 1995). Utrophin is selectively localized at the neuromuscular junction (NMJ), whereas dystrophin is present in the NMJ as well as along the inner face of the surface membrane, the sarcolemma. The DPC seems to contribute to the aggregation of acetylcholine receptors (AChRs) at the NMJ and to enhance the structural stability of the sarcolemma (Grady et al. 2000). Association of signaling molecules, such as nitric oxide synthase, α5β1 integrin, and focal adhesion kinase, with the DPC also suggests a role in signal transduction (Bredt 1999; Hillier et al. 1999; Winder 2001). Disruption of the DPC by

mutations in its main components results in severe muscle dystrophies.

Dystrophin is expressed mainly in skeletal and cardiac muscle and in the brain (Mehler 2000; Blake et al. 2002). Short C-terminal dystrophin isoforms, ranging in size from 71 kDa to 260 kDa and lacking the actin-binding domain, have a more widespread distribution (Ahn and Kunkel 1993; Austin et al. 1995; Sadoulet-Puccio and Kunkel 1996; Durbeej et al. 1997; Culligan et al. 1998; Lidov and Kunkel 1998; Blake et al. 1999, 2002; Lumeng et al. 1999; Chavez et al. 2000). Mice lacking dystrophin and all its C-terminal isoforms including Dp71 (mdx^{3Cv}) are viable, allowing the role of these proteins in non-muscle tissues to be investigated (Cox et al. 1993). Utrophin has a ubiquitous expression pattern, with high levels in lung, kidney, liver, nervous system, and blood vessels (Love et al. 1993; Dixon et al. 1997; Grady et al. 1997a; Tinsley et al. 1998; Rafael et al. 1999; Knuesel et al. 2000; Loh et al. 2000; Raats et al. 2000; Regele et al. 2000; Zuellig et al. 2000; Jimenez-Mallebrera et al. 2003; Haenggi et al. 2004). DPC proteins are molecularly heterogeneous, with the isoforms of each protein being encoded by distinct genes or being generated by alternative splicing or differential promoter usage. In particular, dystrobrevins, which are structurally homologous to dystrophin and utrophin, are encoded by two separate genes, α-dystrobrevin and β-dystrobrevin, the former being alternatively spliced into five distinct isoforms (Blake et al. 1996; Sadoulet-Puccio et al. 1996; Ambrose et al. 1997; Peters et al. 1997b; Nawrotzki et al. 1998; Newey et al. 2001).

The syntrophin family likewise comprises several isoforms in muscle encoded by separate genes (α1, β1, β2) and two brain-specific genes (γ1 and γ2; Piluso et al. 2000; Blake et al. 2002). Whereas sarcoglycans are muscle-specific (Blake et al. 2002), the dystrobrevin and syntrophin isoforms exhibit a differential tissue distribution and are selectively associated with either dystrophin or utrophin, suggesting the existence of several molecularly and functionally distinct DPCs in non-muscle cells.

Analysis of mice with targeted mutations has revealed the interdependence of the DPC with either utrophin or dystrophin for assembly in muscle. For instance, mice with dystroglycan-deficient skeletal muscles and mice lacking α-syntrophin show severely reduced levels of utrophin at the NMJ (Cote et al. 1999; Adams et al. 2000). Conversely, α-dystrobrevins and the syntrophins disappear from the muscle sarcolemma in the absence of dystrophin (mdx mice) but are retained at the NMJ because of their association with utrophin (Deconinck et al. 1997; Grady et al. 1997a; Peters et al. 1997b). The phenotype of utrophin$^{0/0}$ mice has not been investigated in detail. These mice are fertile and exhibit normal behavior and life span. Their NMJ are functionally not altered, although they contain fewer postsynaptic folds possibly because of decreased AChR density (Deconinck et al. 1997; Grady et al. 1997b).

Little is known, however, about the assembly, cellular localization, and function of the DPC in non-muscle tissues. The issue is further complicated because these proteins are not readily detected in morphologically well-preserved tissue, and the molecular composition of the DPC may be cell-type specific (Loh et al. 2000).

The aim of the present study has been to investigate the role of utrophin and the short dystrophin isoform Dp71 for the assembly and subcellular localization of the DPC in the various kidney nephron segments. Dp71 has been reported to represent the main dystrophin isoform in kidney (Lumeng et al. 1999; Loh et al. 2000, 2001). The distribution of DPC proteins was analyzed by high-resolution immunofluorescence staining in wild-type and mutant mice (utrophin$^{0/0}$ and utrophin$^{0/0}$/mdx^{3Cv}). Changes in their expression levels have been assessed by Western blotting experiments. The results reveal a distinct molecular heterogeneity of the DPC in the different segments of the nephron, identified with specific markers. The DPC exhibits a polarized distribution in the basal membrane of tubular epithelial cells in partial dependence on utrophin expression. However, in the absence of utrophin and all dystrophin isoforms in utrophin$^{0/0}$/mdx^{3Cv} mice, the DPC is completely disrupted throughout the nephron, demonstrating that the assembly and/or membrane localization of the complex critically depends on utrophin and Dp71.

Materials and methods

Animals

Utrophin$^{0/0}$ mice were generated by crossing dystrophin–utrophin double-mutants (mdx/utrophin$^{0/0}$, generated on a mixed 129-C57Bl/6 background; Grady et al. 1997a), with wild-type C57Bl/6 mice (Institute of Animal Science, University of Zurich) giving an F1 generation heterozygous for utrophin (utrophin$^{+/0}$; males) or utrophin and dystrophin (mdx: utrophin$^{+/0}$; females). Utrophin$^{0/0}$ mice were obtained by the crossbreeding of heterozygous or homozygous mice. Utrophin$^{0/0}$/mdx^{3Cv} double-knockout mice were generated by crossing utrophin$^{0/0}$ mice with mdx^{3Cv} mice (Jackson Laboratories, Bar Harbor, Me., USA) giving an F1 generation heterozygous for utrophin (utrophin$^{+/0}$; females) and hemizygous for dystrophin (mdx^{3Cv}; males). Utrophin$^{0/0}$/mdx^{3Cv} double-knockout mice were obtained by the crossbreeding of heterozygous mice. For genotyping, DNA from tail biopsies was analyzed by the polymerase chain reaction (PCR). The double-knockout mice lived only 3–4 weeks postpartum. They displayed severe muscle impairment and were smaller by one third than wild-type mice. All animal experiments were approved by the Cantonal Veterinary Office of Zurich. Kidney tissue of α1-syntrophin$^{0/0}$ mice was obtained from Dr. M. Adams, Chapel Hill, N.C., USA.

Immunoblotting

Kidney tissue from adult wild-type and utrophin[0/0] mice was homogenized in 1–2 volumes of ice-cold sucrose buffer (0.32 M sucrose, 10 mM TRIS/HCl pH 7.4, 5 mM EDTA, 0.02% NaN_3, 0.2 mM phenylmethane sulfonyl-fluoride). The homogenate was then made up to ten volumes and centrifuged for 15 min at 1,000g. The supernatant was aliquoted and stored at −80°C.

Crude kidney fractions were subjected to SDS-poly-acrylamide gel electrophoresis (SDS-PAGE) by using 4% stacking and 10% gradient resolving gels. Proteins were transferred onto nitrocellulose membranes (Bio Rad, Reinach, Switzerland) in an electro-blotting apparatus (Trans Blot, Bio Rad, Reinach, Switzerland) at 30 V overnight, at 4°C. For immunodetection, the blots were prepared as described by Knuesel et al. (2000). To quantify changes in protein expression in utrophin[0/0] mice, Western blots were performed with tissue from four mutant and four wild-type animals, with actin as the internal standard.

Immunofluorescence staining

Cryostat sections (12 μm) prepared from fresh-frozen mouse kidney or striated muscle were mounted onto gelatin-coated glass slides, air-dried at room temperature for 30 s, and stored at −20°C. They were thawed at room temperature, immersed in a Petri dish containing 50 ml fixative solution composed of 0.5% paraformaldehyde, 5% Kryofix (Merck, Dietlikon, Switzerland) in 0.15 M phosphate buffer, pH 7.4, irradiated in a microwave oven (30 s at 480 W), and washed twice with phosphate-buffered saline (PBS).

The sections were then incubated overnight at 4°C with primary antibodies diluted in PBS containing 4% normal goat serum (Table 1). Sections were washed extensively in PBS and incubated for 30 min at room temperature with secondary antibodies conjugated to Cy3 (1:500; Jackson ImmunoResearch, West Grove, Pa., USA) or Alexa 488 (1:1,000; Molecular Probes, Eugene, Ore., USA). Sections were washed again, air-dried, and cover-slipped with buffered glycerol.

In control experiments, preadsorption of primary antibodies with peptide antigen (1–10 μg/ml) resulted in a dose-dependent loss of specific immunoreactivity. In double-labeling experiments, omission of one of the primary antibodies during overnight incubation led to complete loss of signal with the corresponding secondary antibodies, indicating the absence of cross-reactivity.

Data analysis

Sections were visualized by epifluorescence microscopy (Zeiss; Jena, Germany), and images were recorded with a digital camera (Orca, Hamamatsu City, Japan). For high magnification imaging, sections were analyzed by laser scanning confocal microscopy (LSM 510 Meta, Zeiss, Jena, Germany) with sequential recording of double-labeled sections to avoid bleed-through between channels.

Table 1 List of antibodies used. Double-immunofluorescence staining experiments were performed with antibodies derived from various species (*aa* amino acid, *a.p.* affinity-purified, *AQP1/2* aquaporin 1/2, *IMF* immunofluorescence, *MRP1/2* multidrug resistant-associated protein 1/2, *NKCC2* Na$^+$–K$^+$–Cl$^-$-cotransporter 2, *WB* Western blotting)

Protein	Antigen/catalog number	Species	Dilution WB	Dilution IMF	Reference/source
Utrophin	aa 1,754–2,089	Guinea pig	1:6,000	1:10,000	Knuesel et al. 2000
		Rabbit	–	1:10,000	
β2-Syntrophin	CSGSEDSGSPKHQTTKDR,	Rabbit	–	1:1,000	Present study
	aa 206–223	(a.p.)	4 μg/ml	4 μg/ml	
		Guinea pig	1:500	1:500	
β1-Syntrophin	CRLGGGSAEPLSSQSFSFHRDR,	Rabbit	–	1:2,000	Present study
	aa 220–240	(a.p.)	4 μg/ml	4 μg/ml	
α1-Syntrophin	CRQPSSPGPQPRNLSEA,	Rabbit	–	1:500	Present study
	aa 191–206	(a.p.)	4 μg/ml	4 μg/ml	
		Guinea pig	–	1:2,000	
Pan-syntrophin	SYN1351E	Mouse	1:10,000	–	Froehner et al. (1987)
Pan-dystrobrevin	βCT-FP	Rabbit a.p.	1:1,000	1:1,000	Blake et al. (1998)
β-Dystroglycan	NCL-b-DG	Mouse	1:2,000	1:100	Novocastra, Newcastle upon Tyne, UK
Dystrophin (Dp71)	Clone 6C5, aa 3,669–3,685	Mouse	1:25	1:100	Anawa trading, Wangen, Switzerland
AQP1	AB3065	Rabbit	–	2 μg/ml	Chemicon Int., Temecula, Calif., USA
AQP2	AB3274	Rabbit	–	1:500	Chemicon Int.
MRP1	SLNKEDTSEEVVPVC, aa 243–256	Guinea pig	–	1:2,000	J.-M. Fritschy, unpublished
MRP2	CEAIESVNHTEL, aa 1,530–1,541	Rabbit	–	1:1,000	J.-M. Fritschy, unpublished
NKCC2	AB3562P	Rabbit	–	1:2,000	Chemicon Int.
Laminin	AB2034	Rabbit	–	1:2,000	Chemicon Int.
Actin	A 2066	Rabbit	–	1:5,000	Fluka Holding, Buchs, Switzerland

The digitized images were processed with the software Imaris 3 (Bitplane, Zurich, Switzerland). Changes in immunofluorescence intensity in tissue from utrophin$^{0/0}$ mice were analyzed by semi-quantitative densitometry in four animals per genotype by using the MCID M5 imaging system (Imaging Research, St-Catherine, ON, Canada). Fluorescent latex beads with relative intensities ranging from 0.1% to 100% were used for calibration (Molecular Probes, Eugene, Ore., USA). For each animal, images were taken under identical conditions at a magnification of 0.07 μm/pixel with a 100× objective (numerical aperture, 1.4). Immunopositive structures were outlined as a region of interest for optical density measurement in single confocal images for ten sections per animal. Data were averaged per animal and statistically compared with the Mann–Whitney test.

## Results

Characterization of antibodies to syntrophin isoforms

Antibodies selectively recognizing α1-syntrophin, β1-syntrophin, or β2-syntrophin (Table 1) were raised by using peptide sequences derived from the first pleckstrin-like domain of rat syntrophin genes (Peters et al. 1994) as antigens. They were tested by immunofluorescence on rat diaphragm (Fig. 1a) and mouse skeletal muscle sections (Fig. 1b, c). β2-Syntrophin immunoreactivity (IR) was most intense at the NMJ (Fig. 1a), whereas β1-syntrophin IR and α1-syntrophin IR was found on the entire sarcolemma (Fig. 1b, c) and at the NMJ (not shown), as expected (Peters et al. 1997a; Adams et al. 2000). In control experiments on kidney sections, specific immuno-fluorescence staining was abolished upon preadsorption of the antisera with their peptide antigen (Fig. 1d–i).

Molecular heterogeneity of the DPC in the nephron

A systematic comparison of the distribution of members of the DPC in relation to specific markers of the main segments of the tubular system revealed a unique pattern for each of these proteins, with a striking regional specificity (Figs. 2, 3, Table 2). Utrophin IR was heterogeneous in the cortex, with glomeruli and isolated tubular segments being most intensely stained (Fig. 2a). These included the cortical thick ascending limbs, which were double-labeled for the Na$^+$–K$^+$–Cl-cotransporter 2 (NKCC2; Payne et al. 1995; Fig. 2b), and connecting


Fig. 1 Specificity test of syntrophin antisera in adult striated muscle **a**, **b**, **c**, and in kidney in the absence **d**, **f**, **h** or presence **e**, **g**, **i** of peptide antigen (5 μg/ml) for competition. Intense β2-syntrophin IR is seen at the neuromuscular junction (NMJ) in adult rat diaphragm (**a**), whereas β1-syntrophin and α1-syntrophin staining outlines the entire sarcolemma in mouse skeletal muscle (**b**, **c**). In kidney, the distinct labeling of medullary tubular epithelial cells, outlining individual tubules, was abolished in preadsorption experiments with β2-syntrophin (**d**, **e**), β1-syntrophin (**f**, **g**), or α1-syntrophin (**h**, **i**). *Bars* 20 μm (**a**), 40 μm (**b**, **c**), 30 μm (**d**–**i**)
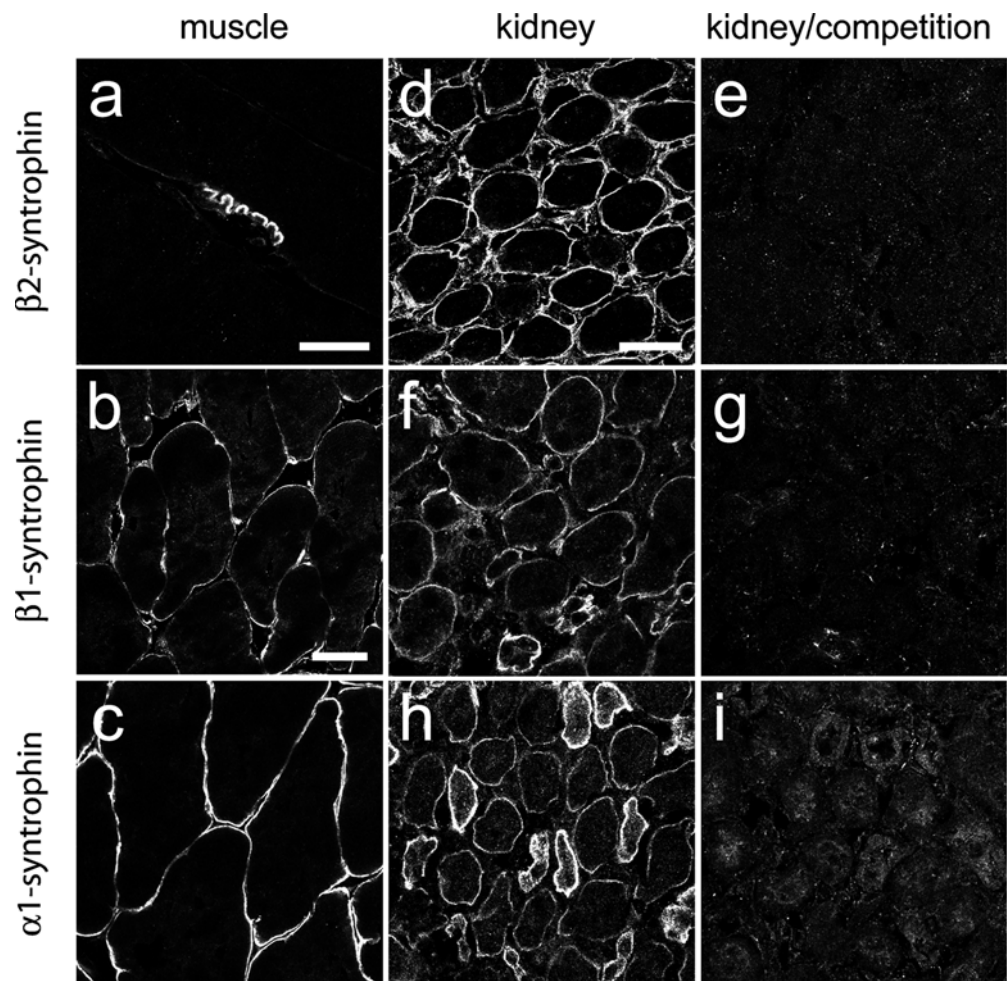
tubules and collecting ducts, which were immunoreactive for aquaporin 2 (AQP2; Nielsen et al. 1993a; Fig. 2c). In contrast, utrophin IR was weak in the proximal tubules, identified with aquaporin 1 (AQP1; Nielsen et al. 1993b;

Fig. 2d) or the multidrug resistant-associated protein 2 (MRP2; not shown). A different pattern was observed in the medulla, where intense utrophin staining homogeneously labeled all tubular segments (Fig. 2e). With the

Fig. 2 Differential localization of utrophin (*green*) in major segments of the nephron identified with specific markers (*red*) in double-immunofluorescence experiments. Mouse kidney cryosections were stained for utrophin (*utro*), either alone (**a**, **e**) or in combination with one of the following markers: Na$^+$/K$^+$/Cl$^-$/cotransporter-2 (*NKCC*; **b**, **f**), aquaporin-2 (*AQP2*; **c**, **g**), aquaporin-1 (*AQP1*; **d**, **h**), multidrug resistant-associated protein-1 (*MRP1*; **i**), and laminin (**k**). Table 2 gives the distribution of these markers. The heterogeneous distribution of utrophin IR in the renal cortex (**a**) is seen at low magnification, with intense staining of glomeruli (*arrowheads*) and isolated tubules. Double-immunofluorescence images allow the identification of the tubules of the cortical thick ascending limbs (**b**) and connecting tubules (**c**), which are intensely stained for utrophin (*green*). In contrast, the proximal tubules (**d**) are only weakly stained for utrophin. In the medulla, utrophin IR is homogeneously distributed (**e**), with intense labeling of the thick ascending limbs (**f**), collecting ducts (**g**), and thin descending limbs (**h**). Vascular bundles, recognized by their intense MRP1 staining appear devoid of utrophin IR (**i**). Double-labeling with laminin (**k**) illustrates the close apposition of utrophin-positive membranes (*green*) with the basal lamina (*red*). *Bars* 200 μm (**a**, **e**, **i**), 30 μm (**b**–**d**), (**f**–**h**), 5 μm (**k**)
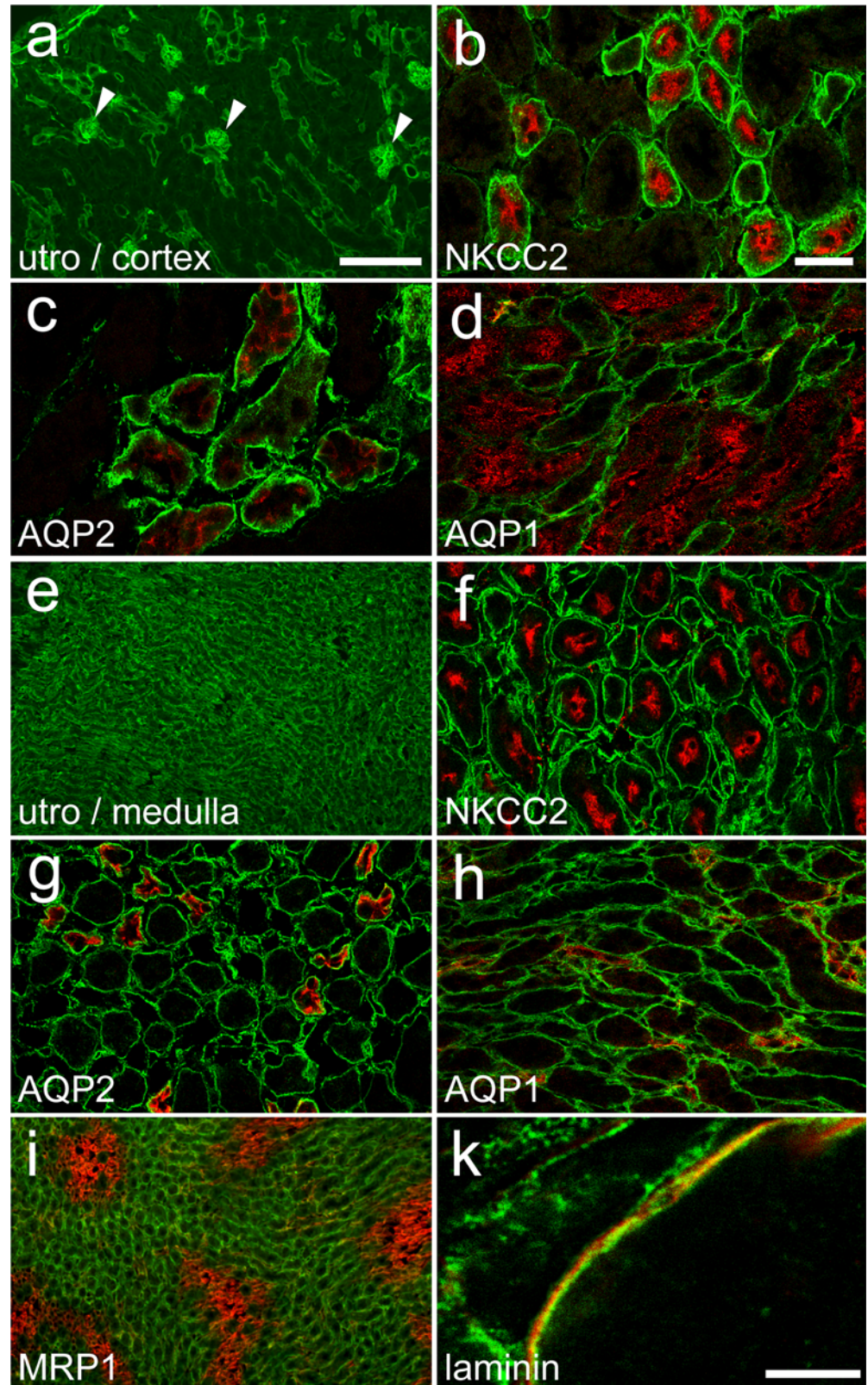
same markers as above (Table 2), utrophin IR was found in medullary thick ascending limbs, which were positive for NKCC2 (Fig. 2f), in the collecting ducts, which were labeled with AQP2 (Fig. 2g), in the descending thin limb of Henle's loop, which was labeled with AQP1-IR (Fig. 2h), and in the ascending thin limbs, distal tubules, and collecting ducts, which were all labeled with MRP1 (Cordon-Cardo et al. 1989; not shown). The only medullary structures lacking utrophin IR were the vascular bundles, which exhibited prominent MRP1 IR (Fig. 2i). At the subcellular level, double-staining with laminin revealed that the two markers were closely apposed but not colocalized (Fig. 2k), suggesting that utrophin IR (green) was restricted to the basal membrane of tubular cells.

The three syntrophin isoforms were colocalized partially with utrophin, but each isoform had a unique distribution pattern (Table 2). In the cortex, β2-syntrophin IR was ubiquitous, being most intense in structures weakly labeled with utrophin, such as the proximal tubules (Table 2). In contrast, the two markers were colocalized in the medulla, outlining all tubules by a strong staining of the basal membrane (Fig. 3a). Like utrophin IR, β2-syntrophin IR was also absent from the medullary vascular bundles. The β1-syntrophin antibody selectively labeled all utrophin-positive tubules in the cortex (Table 2); in the medulla, β1-syntrophin IR was heterogeneous, being

intense in descending thin limbs and collecting ducts, but only weak in thick ascending limbs (Fig. 3b). Finally, α1-syntrophin IR was heterogeneous in the cortex, being restricted to connecting tubules and collecting ducts and always colocalizing with utrophin (Table 2). In the medulla, α1-syntrophin IR differed from β1-syntrophin IR by weaker labeling of the thick ascending limbs and thin descending limbs (Fig. 3c).

The dystrobrevin antibody revealed homogeneous intense staining in the cortex and a heterogeneous pattern in the medulla, with the thick ascending limbs being only weakly labeled (Fig. 3d, Table 2). Although this antibody recognized both α-dystrobrevin and β-dystrobrevin, previous studies indicated that β-dystrobrevin was predominantly expressed in kidney epithelial cells (Kachinsky et al. 1999; Loh et al. 2000, 2001), suggesting that the staining observed here mostly corresponded to this isoform. Taken together, these observations that show syntrophins and dystrobrevin were colocalized with utrophin in the medulla. They could also occur in cortical tubules devoid of utrophin staining (Table 2), where they were presumably associated with dystrobrevin.

Finally, in line with the low abundance of β-dystroglycan and Dp71 reported in kidney (Austin et al. 1995; Durbeej et al. 1997; Tokarz et al. 1998; Durbeej and Campbell 1999; Lumeng et al. 1999; Loh et al. 2000),
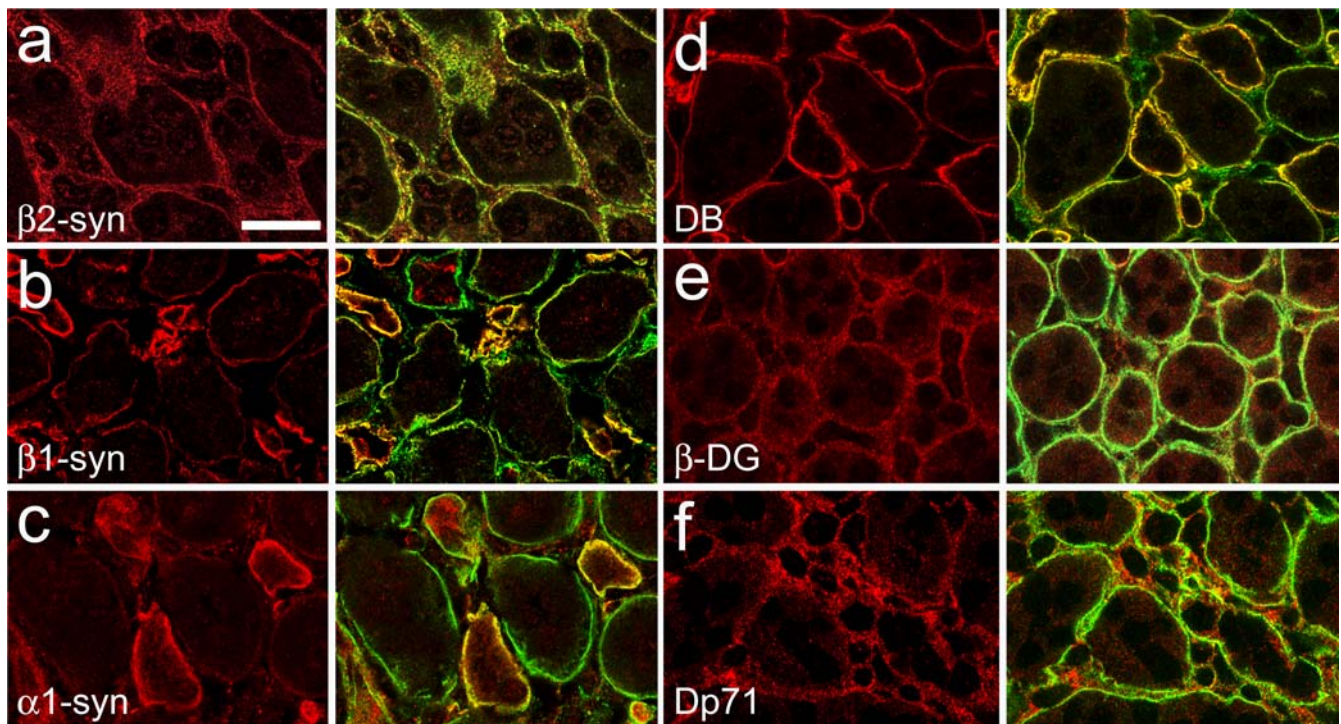

Fig. 3 Subcellular distribution of DPC (*red*) proteins in medullary tubules of wild-type mice (**a–f**) in relation to utrophin (*green*), as seen by double-immunofluorescence staining. In the double-labeled panels, colocalization appears *yellow*. Homogeneous utrophin IR was detected in the basal membrane of medullary thick ascending limbs and collecting ducts, and in small capillaries in the interstitial tissue. Staining for most DPC proteins revealed a precise colocalization with utrophin IR (*yellow*), as shown for β2-syntrophin (**a**, *β2-syn*), β1-syntrophin (**b**, *β1-syn*), α1-syntrophin

(**c**, *α1-syn*), pan-dystrobrevin (**d**, *DB*), and β-dystroglycan (**e**, *β-DG*). In contrast, *Dp71* IR (**f**) was diffuse in the interstitial tissue but was not detectable in tubules, as seen by the lack of colocalization with utrophin (**f**). Tubules weakly labeled with β1-syntrophin, α1-syntrophin, and pan-dystrobrevin were medullary thick ascending limbs, whereas collecting ducts and descending thin limbs were intensely labeled. Note that no dystrobrevin IR was present in the interstitial tissue. *Bar* 20 μm

Table 2 Distribution of DPC proteins in relation to markers (*MRP1/2* multidrug resistant-associated protein 1/2, *NKCC2* $Na^+/K^+/Cl$-cotransporter 2) of the renal tubules (*ATL* ascending thin limbs, *CNT* connecting tubules, *CCT* cortical collecting ducts, *CTAL* cortical thick ascending limbs, *DTL* descending thin limbs, *MCT* medullary collecting ducts, *MTAL* medullary thick ascending limbs, *PT* proximal tubules) and vasculature (*BV* blood vessels) as obtained by double-immunofluorescence staining. Signal intensities were assessed by visual inspection and ranged from background (−) to the most intense staining for each antibody (+++).

Marker	Renal tubules						Vasculature	
	PT	DTL	ATL	MTAL/CTAL	CNT	CCT/MCT	BV	Vascular bundles
Aquaporin 1	+++	+++	−	−	−	−	+	−
Aquaporin 2	−	−	−	−	++	+++	−	−
MRP1	−	−	+++	−	−	−	+++	+++
MRP2	+++	−	−	−	−	−	+++	−
NKCC2	−	−	−	+++	−	−	−	−
Utrophin	+	+++	+++	+++	+++	+++	+++	−
β2-Syntrophin	+++	+++	+++	+++	+++	+++	+++	−
β1-Syntrophin	−	+++	+	+	+++	+++	+++	−
α1-Syntrophin	+	+	+	+	+	+	+++	−
Dystrobrevin	+++	++	++	+	+++	+++	−	−
β-Dystroglycan	+	+	+	+	+	+	+++	++
Dp71	−	−	−	−	−	−	+++	++

immunofluorescence for these proteins appeared weak and diffuse in the nephron (Fig. 3e, f, Table 2). Only glomeruli and blood vessels were intensely stained. β-Dystroglycan staining was moderate in the vascular bundles and isolated capillaries but weaker in medullary tubules; it was however colocalized with utrophin IR (Fig. 3e). Dp71 IR appeared as weak as β-dystroglycan staining (Fig. 3f). However, at high resolution, Dp71 IR clearly outlined interstitial capillaries but was not detectable in the basal membrane of the thick ascending limbs and collecting ducts. The absence of dystrophin was confirmed by the lack of colocalization with utrophin (Fig. 3f). Control experiments were performed in *mdx*[3Cv] mice, in which no specific dystrophin IR was detected (not shown).

In the glomeruli, which stained intensively for both utrophin and Dp71, the two proteins did not colocalize (not shown). Utrophin IR was present in the Bowman's capsule and the intraglomerular convolutes, whereas Dp71 IR was absent from the capsule. The Dp71 antibody stained most prominently in regions toward the macula densa but also bound to intraglomerular structures, a result different from that for utrophin IR. This distribution suggested the presence of utrophin in capsular and intraglomerular epithelial cells and corresponded to electron-microscopic identification of utrophin in a granular podocyte-like staining pattern along the glomerular capillary walls (Raats et al. 2000; Regele et al. 2000). On the other hand, Dp71 seemed to localize to the mesangial and/or endothelial cells, similarly to a particular Dp71 splice variant, Dp71ΔC (Loh et al. 2000). This differential distribution of utrophin and Dp71 corresponded to that observed in the utrophin-positive nephron segments. Glomeruli were not examined in further detail, because specific markers for the various cell types in the glomerulus were not identified, and because the secondary anti-mouse IgGs, used to detect monoclonal antibodies, produced a high background in these structures.

## Alteration of the DPC in kidney of utrophin[0/0] mice

The role of utrophin for the formation of the DPC in the nephron was investigated by analyzing potential alterations in the subcellular distribution of DPC proteins in utrophin[0/0] mice (Fig. 4a–h, Tables 3, 4). The analysis was performed in the medulla, in which the distribution of utrophin was the most homogeneous. Sections from wild-type and mutant mice were processed in parallel under identical conditions and with the same reagents to minimize staining variability. In control experiments, no utrophin staining could be detected in sections from mutant mice, confirming the specificity of the antibody.

Table 3 Alteration of DPC protein IR in utrophin[0/0] mice: comparison of immunofluorescence and Western blot experiments. Quantification of immunohistochemical data and immunoblotting experiments on four wild-type and four utrophin[0/0] mice. Changes in calibrated immunofluorescence intensity were assessed in medullary tubular segments (thick ascending limbs and collecting ducts). Immunoreactive bands in Western blots were measured by using a diffuse density standard curve, and values were normalized to actin levels on the same blots (*NS* not significant). α-Dystrobrevin and β-dystrobrevin could be differentiated in Western blots by their molecular size, but not in the immunofluorescence experiments (pan-dystrobrevin antibody).

DPC proteins	Immunofluorescence (% of wild-type)	Western blot (% of wild-type)
β2-Syntrophin	51±12.2*	77±7.6; NS
β1-Syntrophin	101±0.3; NS	Not quantified
α1-Syntrophin	102±0.2; NS	Not quantified
Pan-dystrobrevin	121±0.9*	–
α-Dystrobrevin	–	114±42.5; NS
β-Dystrobrevin	–	101±10.3; NS
β-Dystroglycan	163±12.6*	60±15.7; NS
Dp71	352±31.4*	260±108*

*$P<0.05$; Mann–Whitney test

Fig. 4 Alterations of DPC protein staining were assessed by using low-resolution confocal images of the renal medulla of wild-type (**a, c, e, g**), utrophin$^{0/0}$ (**b, d, f, h**), and utrophin$^{0/0}$/ mdx^{3Cv} (**i–m**) mice. The images illustrate the reduction of β2-syntrophin IR in utrophin$^{0/0}$ mice (**a, b**) in contrast to the unaltered β1-syntrophin IR and α1-syntrophin IR (**c, d**, and **e, f**, respectively) and to the enhanced dystrobrevin staining, which becomes almost homogeneous because of the increased labeling of the thick ascending limbs (**g, h**). In utrophin$^{0/0}$/mdx^{3Cv} mice, the effects are much more pronounced, and an almost complete loss of staining is observed for β2-syntrophin (**i**), β1-syntrophin (**k**), and dystrobrevin (**m**). Note, however, that α1-syntrophin IR is only partially reduced in the collecting tubules (**l**) in the double-mutant mice. *Bar* 50 μm
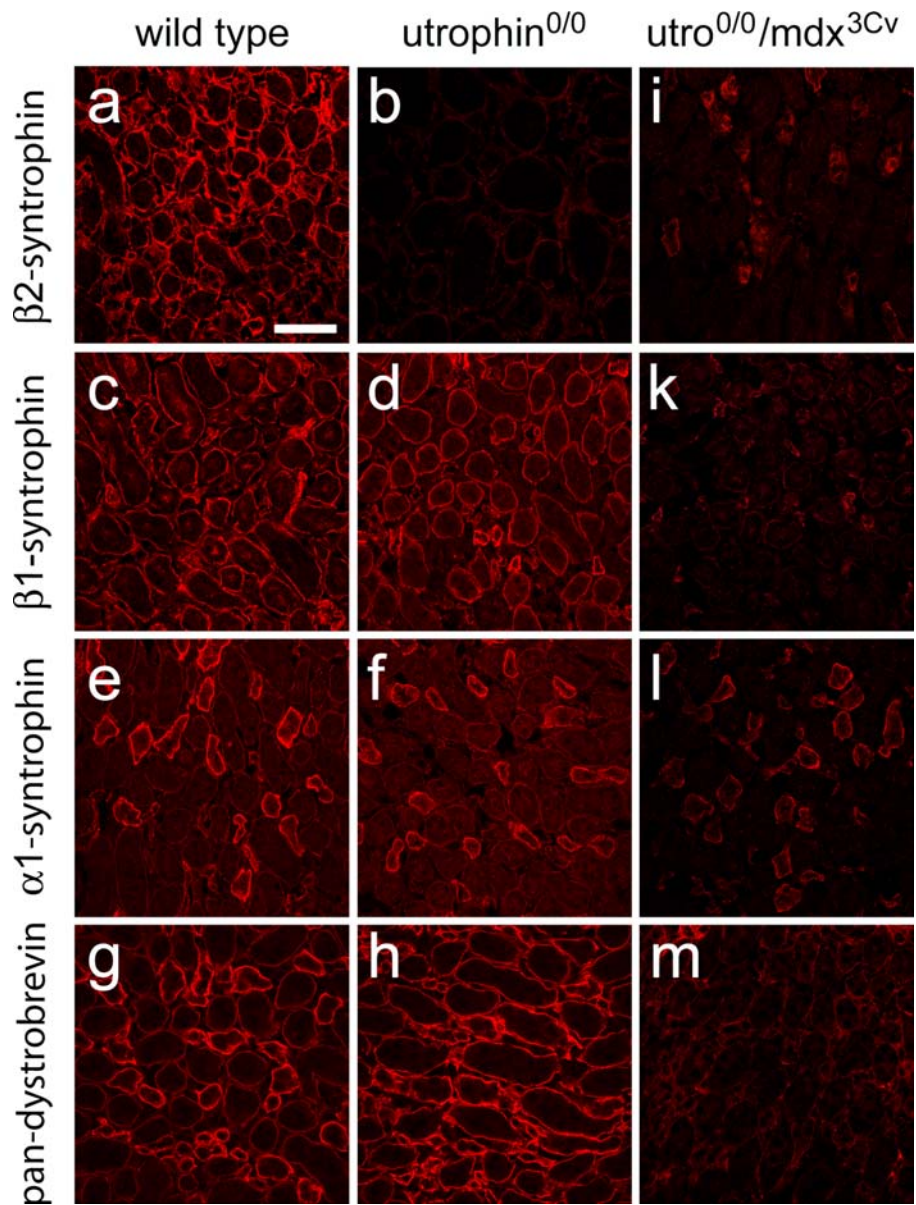
β2-Syntrophin IR was markedly decreased in the medulla of utrophin$^{0/0}$ mice compared with that of the wild-type (Fig. 4a, b). The remaining staining was still localized along the basal membrane of the epithelium in the absence of utrophin (Fig. 4b). This change was highly specific, since β2-syntrophin IR remained unaltered in the

Table 4 Alteration of DPC protein IR in utrophin$^{0/0}$ (*Utro$^{0/0}$*) and utrophin$^{0/0}$/mdx^{3Cv} (*Dko*) mice (*ne* not expressed, *CCT* cortical collecting ducts, *MCT* medullary collecting ducts, *MTAL* medullary thick ascending thin limbs, *PT* proximal tubules). Signal intensities of DPC proteins in specific renal segments were assessed by visual inspection and ranged from not changed (=), to decreased IR (↓), and to no detectable IR (↓↓) on the one hand, and to increased IR (↑) and to strongly increased IR (↑↑) on the other.

| Genotype	Renal segments							
	PT		CCT		MTAL		MCT	
	Utro$^{0/0}$	Dko	Utro$^{0/0}$	Dko	Utro$^{0/0}$	Dko	Utro$^{0/0}$	Dko
β2-Syntrophin	=	↓↓	=	↓↓	↓↓	↓↓	↓↓	↓↓
β1-Syntrophin	=	↓↓	=	↓↓	=	↓↓	=	↓↓
α1-Syntrophin	=	↓	=	↓	=	↓↓	=	↓
Dystrobrevin	=	↓↓	=	↓↓	↑	↓↓	↑	↓↓
Dp71	=	ne	=	ne	↑↑	ne	↑↑	ne

cortex including the glomeruli (not shown), in particular in the proximal tubules in which it was normally not associated with utrophin. In striking contrast, no change in staining intensity or distribution could be observed for β1-syntrophin IR in mutant kidney compared with that of the wild-type (Fig. 4c, d) in tubules of both the cortex and medulla. The same observation was made for α1-syntrophin IR, which was still present in the thick ascending limbs of utrophin-deficient kidney (Fig. 4e, f). These results indicated an obligatory association of β2-syntrophin with utrophin in the membrane of medullary tubular epithelial cells, whereas β1-syntrophin and α1-syntrophin appeared independently of utrophin.

The absence of utrophin also affected β-dystrobrevin staining, but in the opposite direction. Indeed, the heterogeneous labeling seen in the medulla of wild-type mice (Fig. 4g) was replaced by intense homogeneous IR in all thick ascending limbs and collecting ducts (Fig. 4h).

This result suggested that the DPC was partially maintained in the absence of utrophin, possibly by a compensatory increase of β-dystrobrevin IR. When visualized at high magnification, β-dystrobrevin staining clearly was enhanced at the surface of tubules in the utrophin$^{0/0}$ kidney compared with that of the wild-type (Fig. 5a, b). The increased β-dystrobrevin IR therefore was used in double-labeling experiments to determine the localization of β-dystroglycan and Dp71. The former was also increased in the medulla of utrophin$^{0/0}$ mice and was colocalized with β-dystrobrevin (Fig. 5c). Even more striking was the pronounced Dp71 IR in the basal membrane of the collecting ducts and thick ascending limbs in utrophin-deficient kidney; this IR was likewise colocalized with β-dystrobrevin IR (Fig. 5d).

Changes in immunofluorescence staining between mutant and wild-type medulla were quantified by densitometry (Table 3). The measurements were confined to the

Fig. 5 High-resolution images of wild-type (**a**) and utrophin$^{0/0}$ (**b–d**) kidney demonstrating the increased staining of dystrobrevin IR in the basal membrane of the thick ascending tubules (**a**, **b**). Selective colocalization of β-dystroglycan (**c**; *red*) and Dp71 (**d**; *red*) with dystrobrevin (*green*) is indicated in the mutant by *yellow* resulting from the overlay. *Bar* 5 μm
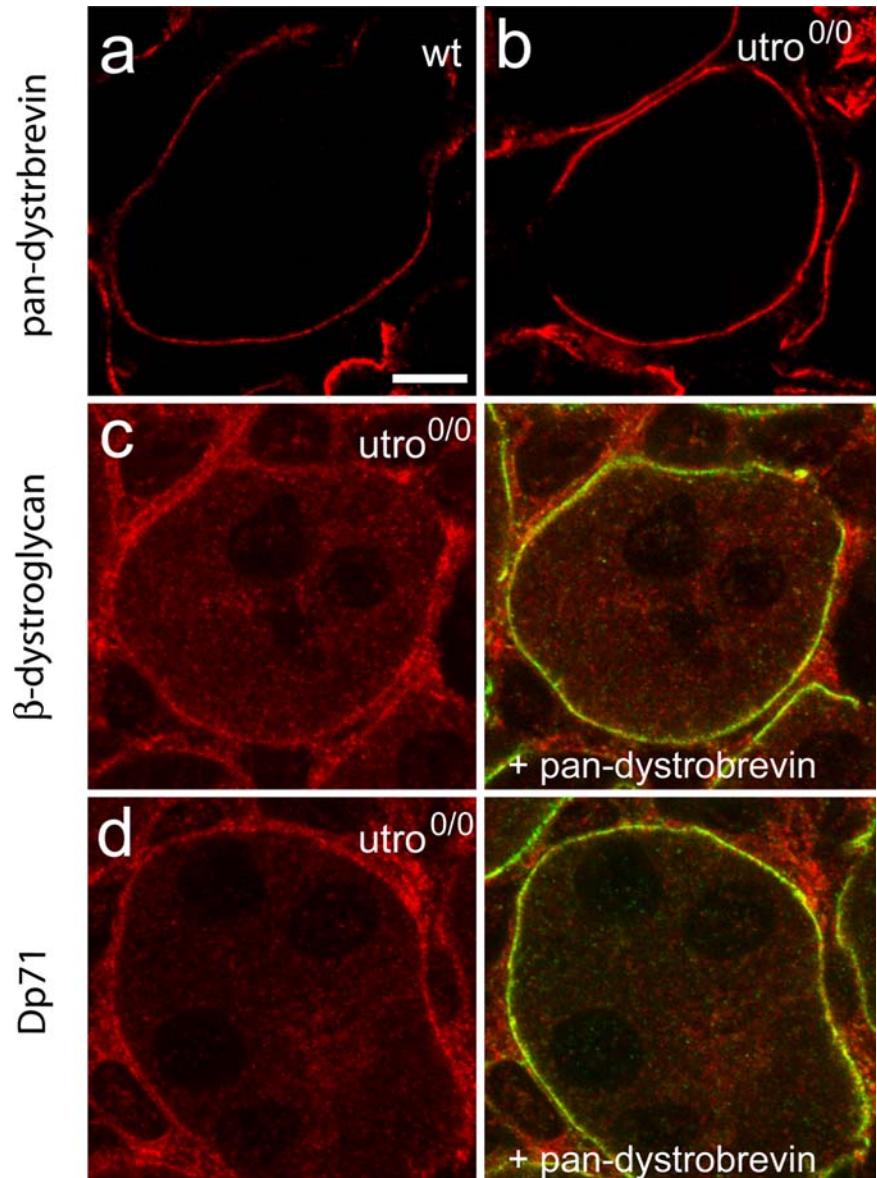
basal membrane of medullary thick ascending limbs and collecting ducts. In wild-type, the cell surface was localized by using utrophin as the reference; in mutants, dystrobrevin IR was used. This analysis revealed an almost 50% decrease in β2-syntrophin IR in mutant kidney and confirmed that β1-syntrophin and α1-syntrophin staining remained unaltered. Dystrobrevin–dystroglycan IR and β-dystroglycan IR were increased by more than 20% and 50%, respectively, in mutant mice, whereas Dp71 IR had more than tripled (Table 3). Taken together, these results indicated that the DPC normally associated with utrophin in medullary tubules had been replaced by a different complex containing β-dystroglycan, Dp71, dystrobrevin, β1-syntrophin, and α1-syntrophin.

Specific upregulation of Dp71 protein expression in utrophin[0/0] mice

The pronounced alterations in immunofluorescence staining observed in utrophin[0/0] mice raised the question as to whether they reflected a change in protein expression or in subcellular localization. Crude kidney extracts prepared from wild-type and utrophin-deficient mice were analyzed by Western blotting (Fig. 6, Table 3). We focused on β2-syntrophin, dystrobrevin, β-dystroglycan, and Dp71, which exhibited differential alterations in immunofluorescence staining. In these experiments, we could discriminate between α1-dystrobrevin and β-dystrobrevin isoforms based on their molecular weight and could show that β-dystrobrevin was more abundant than the α1 isoform (Fig. 6, left panel), confirming previous studies (Blake et al. 1999; Loh et al. 2000).

The increased dystrobrevin and β-dystroglycan immunofluorescence in sections from utrophin[0/0] kidney could not be replicated in the Western blots (Fig. 6, right panel). Conversely, in spite of the profound reduction of β2-syntrophin immunofluorescence, no significant decrease was seen in Western blots (Fig. 6). However, a strong increase in Dp71 protein levels was observed (Fig. 6, Table 3). A compensatory upregulation of this protein might therefore play a crucial role for the maintenance of the DPC in the absence of utrophin.

Disruption of the DPC in kidney of utrophin[0/0]/mdx[3Cv] mice

To verify this hypothesis, we investigated the kidney of double-mutant mice (utrophin[0/0]/mdx[3Cv]) lacking both utrophin and all C-terminal dystrophin isoforms (Fig. 4i–m, Table 4). Most strikingly, the staining of the DPC proteins investigated was largely abolished in tubular epithelial cells and in glomeruli, suggesting that the DPC was not formed in the nephron in the absence of utrophin and Dp71. These results, as illustrated for the medulla (Fig. 4i–m), also provided indirect evidence for the specificity of our antibodies. Unexpectedly, however,
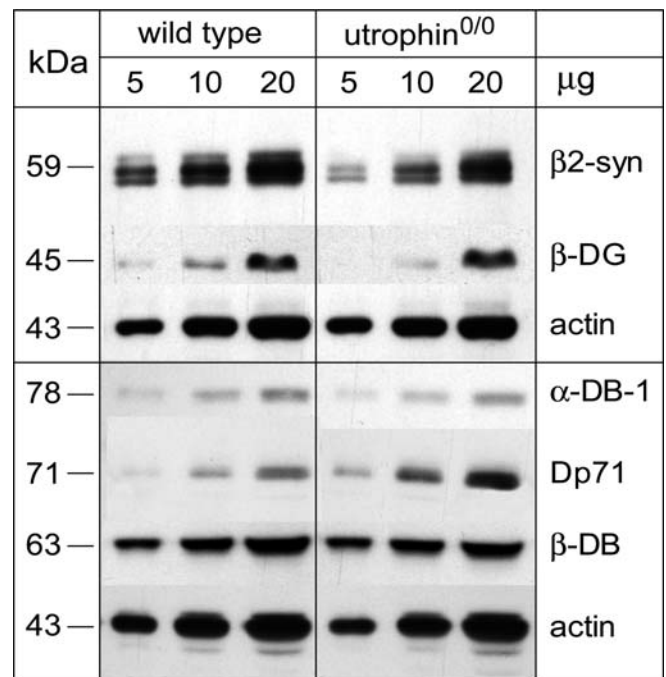

Fig. 6 Semi-quantitative Western blotting of crude kidney extracts from wild-type and utrophin[0/0] mice. Lanes were loaded with 5, 10, and 20 μg protein (*left to right*) and probed with the antibodies indicated *far right*. α-Dystrobrevin-1 (*α-DB-1*; 78 kDa) and β-dystrobrevin (*β-DB*; 63 kDa) were both detected with the pan-dystrobrevin antibody (see Table 1). All lanes were also labeled with antibodies to actin as a control for protein loading and blotting efficiency. No difference in staining intensity was observed between genotypes for β2-syntrophin (*β2-syn*), β-dystroglycan (*β-DG*), α-dystrobrevin-1 (*α-DB-1*) and β-dystrobrevin (*β-DB*). In contrast, staining for *Dp71* was markedly increased in the absence of utrophin. Note the low abundance of α-dystrobrevin compared with β-dystrobrevin in both genotypes. The results of the quantification are given in Table 3.

α1-syntrophin IR was only partially decreased in medullary collecting ducts (Fig. 4l), raising the question as to whether this protein existed alone or whether this staining was an artifact.

Therefore, immunofluorescence experiments were performed in α1-syntrophin[0/0] kidney (Adams et al. 2000). The localization and intensity of the β2-syntrophin IR and β1-syntrophin IR appeared normal in these mice, in both cortex and medulla (Fig. 7). However, the α1-syntrophin staining in the medulla disappeared only from the thick ascending limbs and was partially retained in the collecting ducts (Fig. 7m), as also seen in utrophin[0/0]/mdx[3Cv] mice (Fig. 4l). This result indicated that the α1-syntrophin antibody was not totally specific in this segment of the nephron. Therefore, α1-syntrophin, like the other members of the DPC, did not remain in the cell membrane of tubular epithelial cells in the absence of utrophin and dystrophin. Caution had therefore to be applied to the interpretation of the immunofluorescence experiments, since the non-specific staining in collecting ducts produced by the α1-syntrophin antibody had not been revealed by the preadsorption experiments (Fig. 1i).

Fig. 7 Specificity test of syntrophin antisera in renal cortex and medulla of wild-type (**a**, **c**, **e**, **g**, **i**, **l**) and α1-syntrophin-knockout (α1-syntrophin$^{0/0}$) mouse kidney (**b**, **d**, **f**, **h**, **k**, **m**). β2-Syntrophin (**a**–**d**), β1-syntrophin (**e**–**h**), and α1-syntrophin (**i**–**m**). β2-Syntrophin staining in the cortex (**a**, **b**) and medulla 8**c**, **d**) was identical in both genotypes. The same observation was made for β1-syntrophin staining (**e**–**h**). Unexpectedly, some α1-syntrophin IR was retained in cortical (**i**–**k**) and medullary (**l**, **m**) collecting ducts, whereas the labeling of the remaining structures, in particular the medullary thick ascending limbs was abolished. The antiserum therefore recognized another protein selectively in collecting ducts, in addition to α1-syntrophin. *Bar* 40 μm
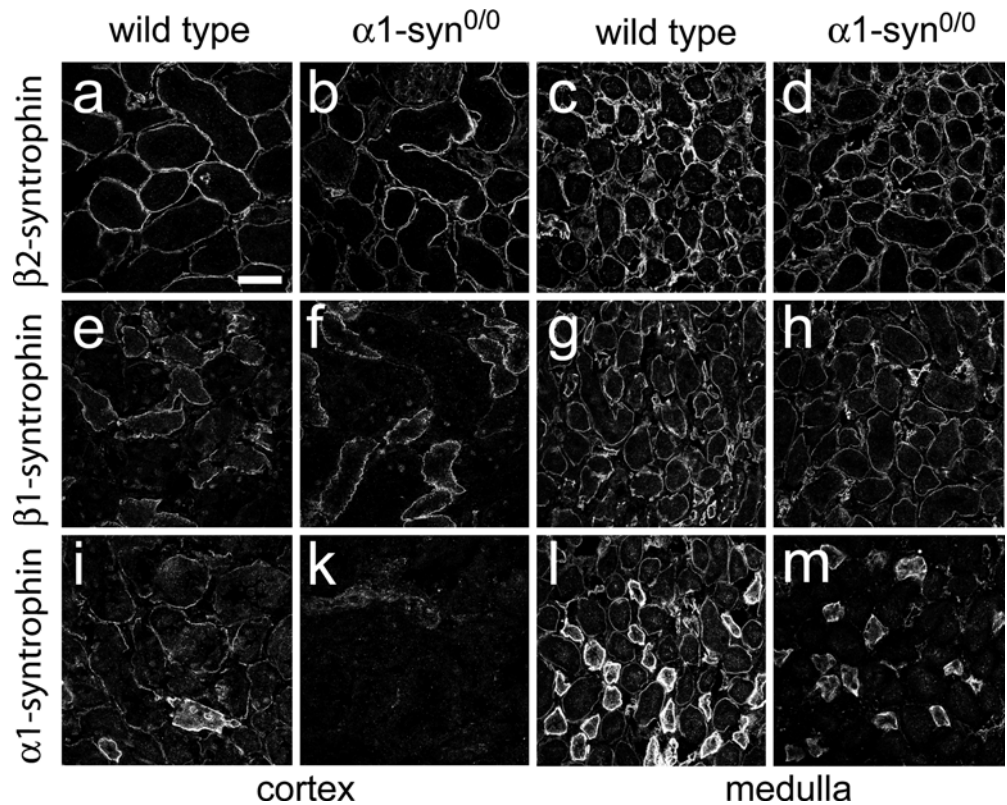
Discussion

The present study provides morphological evidence for the existence of multiple, molecularly distinct DPCs in kidney tubular epithelial cells. This heterogeneity arises from the differential segment-specific distribution of utrophin, dystrobrevin, α1-syntrophin, and β1-syntrophin, whereas β2-syntrophin is present throughout the nephron, together with low levels of β-dystroglycan. In the kidney of utrophin-deficient mice, a profound reorganization takes place, with β2-syntrophin disappearing from the medullary segments, and Dp71 being upregulated and associated with increased levels of β-dystrobrevin and β-dystroglycan. This compensatory mechanism is lost in mice that lack both utrophin and C-terminal dystrophin isoforms and in which the DPC is disrupted throughout the nephron.

These findings reveal a complex interdependence among members of the DPC for assembly and cell-membrane expression. β2-Syntrophin is dependent on utrophin in the medulla but not in the cortex, whereas α1-syntrophin, β1-syntrophin, and dystrobrevin require Dp71 for cell membrane expression. In spite of its homology with dystrophin and utrophin, dystrobrevin cannot form a DPC in kidney tubular epithelial cells in the absence of these partners.

Organization of the DPC in the nephron

We have used segment-specific markers to investigate the organization of the DPC in the nephron and have carried out immunofluorescence experiments on sections weakly fixed by microwave irradiation to minimize loss of antigenicity following fixation (Fritschy et al. 1998). This procedure results in a strong specific immunofluorescence signal, while allowing satisfactory morphological preservation. In contrast, preliminary experiments in perfusion-fixed tissue have revealed only a low signal-to-noise ratio for all DPC proteins tested. The issue of antibody specificity and sensitivity has been a major concern in this study. The almost complete loss of staining seen for all DPC proteins analyzed in double-mutant mice provides an indirect validation of the staining specificity. Although the α1-syntrophin antibody apparently recognizes an additional protein in collecting tubules, this marker is not associated with the cell membrane and does not invalidate our conclusions. With regard to the dystrobrevin isoforms, our results confirm the predominance of β-dystrobrevin over α-dystrobrevins (Fig. 6). Since α-dystrobrevin-1 is present mainly in glomeruli and blood vessels (Loh et al. 2000, 2001), and since α-dystrobrevin-2 is not expressed in kidney (Blake et al. 1996; Loh et al. 2001), the present description of dystrobrevin IR therefore mainly corresponds to β-dystrobrevin.

Our approach has allowed the unambiguous identification of six distinct segments (proximal tubule, descending thin limb, ascending thin limb, thick ascending limb, connecting tubules, and collecting duct) in which the major DPC proteins have been detected (Table 2). The glomerulus has not been analyzed in detail, because the various glomerular cell types could not be identified by

immunofluorescence. In all the staining combinations analyzed in tubular epithelial cells, DPC proteins are precisely colocalized with each other, suggesting that they are part of the same complex. The DPC is probably anchored in the basal membrane, as evidenced by the close apposition of utrophin and laminin. Thus, laminin probably plays an important role in determining the localization of the DPC.

A major finding of this study is that the molecular composition of the DPC is different in each of these six segments of the nephron, because of the differential expression of utrophin, α1-syntrophin, β1-syntrophin, β2-syntrophin, and dystrobrevin. The distal parts of the nephron exhibit strong staining for utrophin, dystrobrevin, and the three syntrophin isoforms. The thick ascending limbs contain mainly utrophin and β2-syntrophin. The proximal tubules mainly contain dystrobrevin together with β2-syntrophin and only little utrophin. The heterogeneity in the expression of the syntrophin isoforms and their differential pattern of coexpression with each other and with dystrobrevin suggest that the molecularly distinct DPCs fulfill distinct functions in the various segments of the nephron.

Finally, the present results confirm that Dp71 is expressed at low protein levels in normal kidney (Lumeng et al. 1999; Loh et al. 2000). The antibody used is directed against the last 17 amino acid residues at the C-terminal of dystrophin and hence recognizes all dystrophin isoforms containing exon 78 (Austin et al. 1995). In addition to Dp71, a larger C-terminal dystrophin isoform, Dp140, has been localized to the basal surface of the tubule epithelium (Lidov and Kunkel 1998). Both Dp71 and Dp140 are reported to occur in kidney in splice variants missing exon 78 (Austin et al. 1995; Lidov and Kunkel 1997; Loh et al. 2000). In both cases, the most C-terminal residues are different in the splice variants and are not recognized by the antibody used here. The splice variant of Dp71, called Dp71ΔC, has been reported to be abundant in the cortex, notably in the proximal tubules, connecting tubules, and collecting ducts (Loh et al. 2000). No information is available concerning Henle's loop and the thick ascending tubules. Dp71ΔC could thus play a role in the assembly of the DPC in those segments of the nephron in which utrophin is scarce.

Alterations of the DPC in utrophin-deficient mice

The analysis of utrophin$^{0/0}$ mice has yielded three distinct results. (1) In the major parts of the nephron, including the proximal tubules, loop of Henle, and collecting ducts, the DPC is not affected by the loss of utrophin. This result could be explained either by the presence of Dp71ΔC or by the upregulation of Dp71. (2) In the thick ascending limb of the medullary tubules, the absence of utrophin leads to a profound reduction of β2-syntrophin IR; this is not a result of the disruption of the DPC, since the other syntrophin isoforms remain unchanged, and since dystrobrevin staining is enhanced. Therefore, in a DPC contain-

ing only low levels of dystrobrevin, β2-syntrophin appears to depend on utrophin for association with the DPC. (3) The loss of utrophin is compensated by the upregulation of Dp71 and increased staining for β-dystroglycan and β-dystrobrevin; the resulting DPC is molecularly distinct from that formed in wild-type mice, but its polarized distribution in the basal membrane is fully retained.

Our Western blot analysis demonstrates that only the expression of Dp71 is upregulated in utrophin$^{0/0}$ mice, whereas the total protein levels of dystrobrevin and syntrophins remain largely unchanged, in spite of the prominent changes in immunoreactivity observed. Although immunoblot analysis of the entire kidney lacks spatial selectivity, this observation points to the existence of an intracellular pool of DPC proteins, independent of the membrane-associated complex in epithelial cells. The absence of utrophin might merely change the affinity of DPC proteins for the complex, thereby shifting the equilibrium between the DPC and the intracellular pool. Apparently, the "unused" β2-syntrophin is not degraded, since this protein is present at comparable levels in wild-type and utrophin$^{0/0}$ mice.

Role of utrophin and Dp71 for the formation of the DPC

The classical model of the DPC in muscle cells postulates that dystrophin or utrophin is essential for the assembly of the complex, but that these two proteins are, at least in part, functionally interchangeable (Blake and Martin-Rendon 2002). This view has mainly been derived from the analysis of *mdx* and *mdx*/utrophin$^{0/0}$ mice, which exhibit strongly reduced levels of dystrobrevins and syntrophins in the sarcolemma and the NMJ, and from the demonstration that the retention of dystrophin in utrophin$^{0/0}$ mice is sufficient to prevent any deleterious effects on other DPC proteins (Blake and Martin-Rendon 2002). On the other hand, ablation of a DPC component such as α-dystrobrevin affects neither dystrophin nor utrophin, whereas the syntrophins are concomitantly reduced (Grady et al. 2000). However, ablation of α1-syntrophin leads to the loss of utrophin at the NMJ, whereas β1-syntrophin in the sarcolemma and β2-syntrophin in the NMJ are significantly upregulated (Adams et al. 2000). The role of syntrophins has further been examined in polarized epithelial cells in vitro, demonstrating the essential role of a highly conserved C-terminal domain for utrophin binding and membrane targeting (Kachinsky et al. 1999).

In non-muscle cells, the situation is more complex, and no clear rules have yet emerged. Loh et al. (2000) have demonstrated that the absence of all dystrophin isoforms in *mdx*^{3Cv} mice has no effect on the distribution of DPC proteins, except that β2-syntrophin is profoundly reduced in glomeruli and cortical renal tubules. Furthermore, inactivation of the β-dystrobrevin gene results in a profound loss of Dp71 and syntrophins, whereas α-dystrobrevin and utrophin are not altered (Loh et al. 2001).

Loh et al. (2001) have concluded that β-dystrobrevin represents a key organizer of the DPC in kidney.

All told, these results indicate that Dp71 and possibly other dystrophin isoforms, together with α-dystrobrevin and β-dystrobrevin, have different roles in muscle and non-muscle tissues with respect to the assembly of the DPC. It is not established, however, whether this disparity is attributable to functional differences between the isoforms, to differences in the molecular composition of the DPC (for instance, dystroglycan is less abundant in kidney than in muscle), or to potential redundancies with other DPC proteins. Our findings in double-mutant mice indicate that the DPC is disrupted in the absence of both dystrophin and utrophin. The implications may be that the mild changes seen in utrophin$^{0/0}$ mice are attributable to the presence of Dp71ΔC in the cortex and to the upregulation of Dp71 in the medulla. Furthermore, these results show that β-dystrobrevin, in spite of its homology with dystrophin and utrophin, cannot form a DPC without one of these partners. Recently, we have shown that both utrophin and Dp71 play an essential role for assembly of the DPC also in the cerebrospinal fluid- and blood brain barriers (Haenggi et al. 2004).

Functional consequences

Utrophin$^{0/0}$/*mdx*^{3Cv} double-mutant mice do not exhibit a devastating pathology in non-muscle tissues (Rafael et al. 1999). The DPC does not appear essential for normal embryogenesis and development of the kidney or presumably for its basic function in laboratory animals. This conclusion does not exclude impaired function under specific conditions and/or the activation of compensatory mechanisms to maintain the function of tubular epithelial cells. Indeed, Loh et al. (2001) have shown that the glucose/creatine ratio in urine samples from female β-dystrobrevin-deficient females mice is increased. Since glucose transporter protein 1 is localized in the basolateral membrane of the epithelium of the renal collecting duct (Farrell et al. 1992), the DPC may contribute to the anchoring of this transporter to the membrane of collecting ducts and possibly to the polarized distribution of a vast array of membrane proteins. In addition, the molecular heterogeneity of the DPC along the main segments of the nephron strongly suggests a functional specialization. Since syntrophins have the potential to bind to various proteins containing a PDZ-domain (Peters et al. 1997a; Albrecht and Froehner 2002), the DPC may mediate specialized signaling functions in kidney epithelial cells. One might therefore expect alterations in signal transduction in utrophin$^{0/0}$/*mdx*^{3Cv} mice.

Conclusions

The DPC has been localized to the basal membranes of the epithelial cells of the nephron, and its composition appears to differ specifically with respect to the various tubular segments. In the absence of utrophin, the DPC changes its composition and associates with Dp71, which seems to replace utrophin at the inner side of the cell membrane. Upon ablation of not only Dp71, but also all C-terminal dystrophin isoforms in addition to utrophin, the DPC disintegrates completely. The double-knockout mice studied display a fragile phenotype resulting in death after 3–4 weeks postpartum. Our new findings suggest that these animals, in addition to muscle disturbances, also suffer from impaired kidney function.

References

Adams ME, Kramarcy N, Krall SP, Rossi SG, Rotundo RL, Sealock R, Froehner SC (2000) Absence of α-syntrophin leads to structurally aberrant neuromuscular synapses deficient in utrophin. J Cell Biol 150:1385–1398

Ahn AH, Kunkel LM (1993) The structural and functional diversity of dystrophin. Nat Genet 3:283–291

Albrecht DE, Froehner SC (2002) Syntrophins and dystrobrevins: defining the dystrophin scaffold at synapses. Neurosignals 11:123–129

Ambrose HJ, Blake DJ, Nawrotzki RA, Davies KE (1997) Genomic organization of the mouse dystrobrevin gene: comparative analysis with the dystrophin gene. Genomics 39:359–369

Austin RC, Howard PL, D'Souza VN, Klamut HJ, Ray PN (1995) Cloning and characterization of alternatively spliced isoforms of Dp71. Hum Mol Genet 4:1475–1483

Blake DJ, Martin-Rendon E (2002) Intermediate filaments and the function of the dystrophin–protein complex. Trends Cardiovasc Med 12:224–228

Blake DJ, Nawrotzki R, Peters MF, Froehner SC, Davies KE (1996) Isoform diversity of dystrobrevin, the murine 87-kDa postsynaptic protein. J Biol Chem 271:7802–7810

Blake DJ, Nawrotzki R, Loh NY, Gorecki DC, Davies KE (1998) β-Dystrobrevin, a member of the dystrophin-related protein family. Proc Natl Acad Sci USA 95:241–246

Blake DJ, Hawkes R, Benson MA, Beesley PW (1999) Different dystrophin-like complexes are expressed in neurons and glia. J Cell Biol 147:645–658

Blake DJ, Weir A, Newey SE, Davies KE (2002) Function and genetics of dystrophin and dystrophin-related proteins in muscle. Physiol Rev 82:291–329

Bredt DS (1999) Knocking signalling out of the dystrophin complex. Nat Cell Biol 1:E89–E91

Chavez O, Harricane MC, Aleman V, Dorbani L, Larroque C, Mornet D, Rendon A, Martinez-Rojas D (2000) Mitochondrial expression of a short dystrophin-like product with molecular weight of 71 kDa. Biochem Biophys Res Commun 274:275–280

Cordon-Cardo C, O'Brien JP, Casals D, Rittman-Grauer L, Biedler JL, Melamed MR, Bertino JR (1989) Multidrug-resistance gene (P-glycoprotein) is expressed by endothelial cells at blood-brain barrier sites. Proc Natl Acad Sci USA 86:695–698

Cote PD, Moukhles H, Lindenbaum M, Carbonetto S (1999) Chimaeric mice deficient in dystroglycans develop muscular dystrophy and have disrupted myoneural synapses. Nat Genet 23:338–342

Cox GA, Phelps SF, Chapman VM, Chamberlain JS (1993) New mdx mutation disrupts expression of muscle and nonmuscle isoforms of dystrophin. Nat Genet 4:87–93

Culligan KG, Mackey AJ, Finn DM, Maguire PB, Ohlendieck K (1998) Role of dystrophin isoforms and associated proteins in muscular dystrophy (review). Int J Mol Med 2:639–648

Deconinck AE, Potter AC, Tinsley JM, Wood SJ, Vater R, Young C, Metzinger L, Vincent A, Slater CR, Davies KE (1997) Postsynaptic abnormalities at the neuromuscular junctions of utrophin-deficient mice. J Cell Biol 136:883–894

Dixon AK, Tait TM, Campbell EA, Bobrow M, Roberts RG, Freeman TC (1997) Expression of the dystrophin-related protein 2 (Drp2) transcript in the mouse. J Mol Biol 270:551–558

Durbeej M, Campbell KP (1999) Biochemical characterization of the epithelial dystroglycan complex. J Biol Chem 274:26609–26616

Durbeej M, Jung D, Hjalt T, Campbell KP, Ekblom P (1997) Transient expression of Dp140, a product of the Duchenne muscular dystrophy locus, during kidney tubulogenesis. Dev Biol 181:156–167

Farrell CL, Yang J, Pardridge WM (1992) GLUT-1 glucose transporter is present within apical and basolateral membranes of brain epithelial interfaces and in microvascular endothelia with and without tight junctions. J Histochem Cytochem 40:193–199

Fritschy JM, Weinmann O, Wenzel A, Benke D (1998) Synapse-specific localization of NMDA and GABA(A) receptor subunits revealed by antigen-retrieval immunohistochemistry.J Comp Neurol 390:194–210

Froehner SC, Murnane AA, Tobler M, Peng HB, Sealock R (1987) A postsynaptic Mr 58,000 (58 K) protein concentrated at acetylcholine receptor-rich sites in Torpedo electroplaques and skeletal muscle. J Cell Biol 104:1633–1646

Grady RM, Merlie JP, Sanes JR (1997a) Subtle neuromuscular defects in utrophin-deficient mice. J Cell Biol 136:871–882

Grady RM, Teng H, Nichol MC, Cunningham JC, Wilkinson RS, Sanes JR (1997b) Skeletal and cardiac myopathies in mice lacking utrophin and dystrophin: a model for Duchenne muscular dystrophy. Cell 90:729–738

Grady RM, Zhou H, Cunningham JM, Henry MD, Campbell KP, Sanes JR (2000) Maturation and maintenance of the neuromuscular synapse: genetic evidence for roles of the dystrophin–glycoprotein complex. Neuron 25:279–293

Haenggi T, Soontornmalai A, Schaub MC, Fritschy JM (2004) The role of utrophin and Dp71 for assembly of different dystrophin-associated protein complexes (DPCs) in the choroid plexus and microvasculature of the brain. Neuroscience 129:403–413

Hillier BJ, Christopherson KS, Prehoda KE, Bredt DS, Lim WA (1999) Unexpected modes of PDZ domain scaffolding revealed by structure of nNOS–syntrophin complex. Science 284:812–815

Jimenez-Mallebrera C, Davies K, Putt W, Edwards YH (2003) A study of short utrophin isoforms in mice deficient for full-length utrophin. Mamm Genome 14:47–60

Kachinsky AM, Froehner SC, Milgram SL (1999) A PDZ-containing scaffold related to the dystrophin complex at the basolateral membrane of epithelial cells. J Cell Biol 145:391–402

Knuesel I, Bornhauser BC, Zuellig RA, Heller F, Schaub MC, Fritschy JM (2000) Differential expression of utrophin and dystrophin in CNS neurons: an in situ hybridization and immunohistochemical study. J Comp Neurol 422:594–611

Lidov HG, Kunkel LM (1997) Dp140: alternatively spliced isoforms in brain and kidney. Genomics 45:132–139

Lidov HG, Kunkel LM (1998) Dystrophin and Dp140 in the adult rodent kidney. Lab Invest 78:1543–1551

Loh NY, Newey SE, Davies KE, Blake DJ (2000) Assembly of multiple dystrobrevin-containing complexes in the kidney. J Cell Sci 113:2715–2724

Loh NY, Nebenius-Oosthuizen D, Blake DJ, Smith AJ, Davies KE (2001) Role of β-dystrobrevin in nonmuscle dystrophin-associated protein complex-like complexes in kidney and liver. Mol Cell Biol 21:7442–7448

Love DR, Byth BC, Tinsley JM, Blake DJ, Davies KE (1993) Dystrophin and dystrophin-related proteins: a review of protein and RNA studies. Neuromuscul Disord 3:5–21

Lumeng CN, Hauser M, Brown V, Chamberlain JS (1999) Expression of the 71 kDa dystrophin isoform (Dp71) evaluated by gene targeting. Brain Res 830:174–178

Matsumura K, Ervasti JM, Ohlendieck K, Kahl SD, Campbell KP (1992) Association of dystrophin-related protein with dystrophin-associated proteins in mdx mouse muscle. Nature 360:588–591

Mehler MF (2000) Brain dystrophin, neurogenetics and mental retardation. Brain Res Brain Res Rev 32:277–307

Nawrotzki R, Loh NY, Ruegg MA, Davies KE, Blake DJ (1998) Characterisation of α-dystrobrevin in muscle. J Cell Sci 111:2595–2605

Newey SE, Gramolini AO, Wu J, Holzfeind P, Jasmin BJ, Davies KE, Blake DJ (2001) A novel mechanism for modulating synaptic gene expression: differential localization of α-dystrobrevin transcripts in skeletal muscle. Mol Cell Neurosci 17:127–140

Nielsen S, DiGiovanni SR, Christensen EI, Knepper MA, Harris HW (1993a) Cellular and subcellular immunolocalization of vasopressin-regulated water channel in rat kidney. Proc Natl Acad Sci USA 90:11663–11667

Nielsen S, Smith BL, Christensen EI, Knepper MA, Agre P (1993b) CHIP28 water channels are localized in constitutively water-permeable segments of the nephron. J Cell Biol 120:371–383

Payne JA, Xu JC, Haas M, Lytle CY, Ward D, Forbush B III (1995) Primary structure, functional expression, and chromosomal localization of the bumetanide-sensitive Na–K–Cl cotransporter in human colon. J Biol Chem 270:17977–17985

Peters MF, Kramarcy NR, Sealock R, Froehner SC (1994) β2-Syntrophin: localization at the neuromuscular junction in skeletal muscle. Neuroreport 5:1577–1580

Peters MF, Adams ME, Froehner SC (1997a) Differential association of syntrophin pairs with the dystrophin complex. J Cell Biol 138:81–93

Peters MF, O'Brien KF, Sadoulet-Puccio HM, Kunkel LM, Adams ME, Froehner SC (1997b) β-Dystrobrevin, a new member of the dystrophin family. Identification, cloning, and protein associations. J Biol Chem 272:31561–31569

Piluso G, Mirabella M, Ricci E, Belsito A, Abbondanza C, Servidei S, Puca AA, Tonali P, Puca GA, Nigro V (2000) γ1- and γ2-syntrophins, two novel dystrophin-binding proteins localized in neuronal cells. J Biol Chem 275:15851–15860

Raats CJ, Born J van den, Bakker MA, Oppers-Walgreen B, Pisa BJ, Dijkman HB, Assmann KJ, Berden JH (2000) Expression of agrin, dystroglycan, and utrophin in normal renal tissue and in experimental glomerulopathies. Am J Pathol 156:1749–1765

Rafael JA, Trickett JI, Potter AC, Davies KE (1999) Dystrophin and utrophin do not play crucial roles in nonmuscle tissues in mice. Muscle Nerve 22:517–519

Regele HM, Fillipovic E, Langer B, Poczewki H, Kraxberger I, Bittner RE, Kerjaschki D (2000) Glomerular expression of dystroglycans is reduced in minimal change nephrosis but not in focal segmental glomerulosclerosis. J Am Soc Nephrol 11:403–412

Sadoulet-Puccio HM, Kunkel LM (1996) Dystrophin and its isoforms. Brain Pathol 6:25–35

Sadoulet-Puccio HM, Khurana TS, Cohen JB, Kunkel LM (1996) Cloning and characterization of the human homologue of a dystrophin related phosphoprotein found at the Torpedo electric organ post-synaptic membrane. Hum Mol Genet 5:489–496

Tinsley J, Deconinck N, Fisher R, Kahn D, Phelps S, Gillis JM, Davies K (1998) Expression of full-length utrophin prevents muscular dystrophy in mdx mice. Nat Med 4:1441–1444

Tokarz SA, Duncan NM, Rash SM, Sadeghi A, Dewan AK, Pillers DA (1998) Redefinition of dystrophin isoform distribution in mouse tissue by RT-PCR implies role in nonmuscle manifestations of Duchenne muscular dystrophy. Mol Genet Metab 65:272–281

Way M, Pope B, Cross RA, Kendrick-Jones J, Weeds AG (1992) Expression of the N-terminal domain of dystrophin in *E. coli* and demonstration of binding to F-actin. FEBS Lett 301:243–245

Winder SJ (2001) The complexities of dystroglycan. Trends Biochem Sci 26:118–124

Winder SJ, Hemmings L, Maciver SK, Bolton SJ, Tinsley JM, Davies KE, Critchley DR, Kendrick-Jones J (1995) Utrophin actin binding domain: analysis of actin binding and cellular targeting. J Cell Sci 108:63–71

Zuellig RA, Bornhauser BC, Knuesel I, Heller F, Fritschy JM, Schaub MC (2000) Identification and characterisation of transcript and protein of a new short N-terminal utrophin isoform. J Cell Biochem 77:418–431